Acta Crystallographica Section D
Biological Crystallography
ISSN 0907-4449

Crystallization and preliminary X-ray analysis of native and selenomethionine fructose-1,6-bisphosphate aldolase from *Thermus aquaticus*

Véronique Sauvé† and Jurgen Sygusch*

Département de Biochimie, Université de Montréal, C.P. 6128, Succursale Centre-Ville, Montréal H3C 3J7, Canada

† Present address: Biotechnology Research Institute, National Research Council of Canada, 6100 Avenue Royalmount, Montréal H4P 2R2, Canada.

Correspondence e-mail: jurgen.sygusch@umontreal.ca

Received 1 September 2000
Accepted 5 December 2000

Fructose-1,6-bisphosphate aldolase (E.C. 4.1.2) catalyses the reversible cleavage of fructose-1,6-bisphosphate to dihydroxyacetone phosphate and glyceraldehyde-3-phosphate in the glycolytic pathway of prokaryote and eukaryote organisms. The enzyme was obtained from the extreme thermophile *Thermus aquaticus* and, in contrast to mesophilic aldolases, expresses maximal activity in the presence of Co^{2+} as cofactor instead of Zn^{2+}. The purified recombinant protein was monodisperse according to dynamic light-scattering measurements. Crystals of recombinant native class II fructose-1,6-bisphosphate aldolase from *T. aquaticus* were obtained from two different starting conditions at low protein concentrations. Condition I, using the sitting-drop vapour-diffusion method, yielded monoclinic crystals having space group $P2$ and unit-cell parameters a = 99.5, b = 57.5, c = 138.6 Å, β = 90.25°. Diffraction data were collected to 2 Å resolution at beamline X8-C of the NSLS synchrotron-radiation source. Native and selenomethionine-substituted protein crystals were obtained from condition II by hanging-drop vapor diffusion. The tetragonal crystals of the native protein belong to the space group $P4_1$, with unit-cell parameters $a = b$ = 88.8, c = 163.1 Å, while those of the SeMet protein have space group $I4_1$, with unit-cell parameters $a = b$ = 88.6, c = 164.1 Å. A data set suitable for MAD phasing was collected to 2.6 Å resolution at beamline X8-C of the NSLS synchrotron source.

1. Introduction

Aldolases have been the subject of continuous interest because they provide a mechanism for carbon–carbon bond formation in living organisms. Fructose-1,6-bisphosphate aldolases (E.C. 4.1.2) are enzymes involved in glycolysis, where they reversibly catalyze cleavage of fructose-1,6-bisphosphate (FBP) to yield dihydroxyacetone phosphate and glyceraldehyde-3-phosphate, or used in gluconeogenesis and the Calvin cycle, where they catalyze the reverse condensation reaction. The FBP aldolases can be divided into two classes. In class I enzymes, found mainly in higher organisms, aldolases use in their reaction mechanism a lysine at their active site to form a Schiff base with substrate. Class II enzymes are metalloenzymes that require a bivalent metal cation for catalysis and are found primarily in lower organisms (Rutter, 1964). Class II enzymes can be subdivided into two subclasses, A and B, according to alignment of their amino-acid sequence (Plaumann *et al.*, 1997). Class II A brings together the glycolytic enzymes from ε- and γ-proteobacteria (such as *Escherichia* and *Campylobacter*, respectively), Gram-positive bacteria with high C/G content (*Mycobacterium*) and eukaryotes (yeast). Class II B aldolases make up the Calvin cycle enzymes from α- and β-proteobacteria (*Synechocystis* and *Rhodobacter*), glycolytic and gluconeogenetic enzymes from Gram-positive bacteria with low C/G content (*Bacillus*), extremophile aldolases (*Thermus*, *Helicobacter*, *Thermotoga*) and proteobacterial aldolases using other substrates (tagatose-1,6-bisphosphate in *E. coli*).

Structures of three class II aldolases, each of different specificities, have been determined so far. Polypeptide folding and metal-cofactor utilization vary among the mesophilic aldolases. The first structure solved was that of *E. coli* L-fuculose-1-phosphate aldolase, a zinc-binding homotetramer of 23.7 kDa subunits (Dreyer & Schulz, 1993). Its fold corresponds to a central nine-stranded β-pleated sheet surrounded by two helices on each side of the sheet, with an active site located at the subunit interface. The catalytic zinc ion is coordinated by three histidines and a glutamic acid in the absence of substrate (Dreyer & Schulz, 1993). The polypeptide folding of the homodimeric class II A FBP aldolase from the mesophile *E. coli* corresponds to an $(\alpha/\beta)_8$ barrel, a form

also observed in class I FBP aldolases, but in this case the active site is located proximal to the C-terminal end of the barrel (Blom *et al.*, 1996; Cooper *et al.*, 1996). The active site contains two distinct but exclusive positions for zinc binding (Blom *et al.*, 1996). In the buried position, zinc is chelated, as in fuculose-1-phosphate aldolase, by three histidine residues and one glutamate residue. At the surface position, the histidines rotate allowing zinc binding with phosphoglycolohydroxamate (Hall *et al.*, 1999) or two water molecules in the absence of substrate (Blom *et al.*, 1996). The active site also has a monovalent cation site in which the cation aligns an aspartic acid that may be involved in the carbon–carbon bond-forming step of the reaction (Plater *et al.*, 1999). More recently, the structure of *E. coli* 2-dehydro-3-deoxy-galactarate aldolase was solved (Izard & Blackwell, 2000). The active form of this enzyme is a hexamer having 27.4 kDa identical subunits that use a divalent metal ion capable of octahedral coordination such as magnesium to promote catalysis. The polypeptide fold is that of a modified $(\alpha/\beta)_8$ barrel in which the last helix is oriented away from the β-barrel instead of packing against it.

To date, the structure of a thermophilic aldolase has yet to be determined. Thermophilic organisms represent an extreme adaptation by life and can be deeply rooted in the eubacterial evolutionary tree (Woese, 1987). Their adaptation to high temperature appears to be subtle, as the proteins do not exhibit significant amino-acid differences with respect to their mesophilic homologues. Differences consist of a rather limited number of additional hydrogen bonds, ion pairs or hydrophobic interactions to augment thermostability (Haney *et al.*, 1999).

T. aquaticus YT-1 (*Taq*) is a Gram-negative thermophilic eubacteria that was first isolated from the hot springs (343 K) of Yellowstone Park (Brock & Freeze, 1969) and has become famous because of its DNA polymerase used in PCR. Comparisons with FBP aldolase amino-acid sequences indicate that the FBP aldolase sequence from *T. aquaticus* YT-1 is similar to those of class II B FBP aldolases (Sauvé & Sygusch, 2001). The *Taq* aldolase enzyme differs from the dimeric *E. coli* class II FBP aldolase, which prefers divalent zinc as metal cofactor while the *Taq* aldolase displays highest activity in presence of divalent cobalt cation. Also, the quaternary structure of the *Taq* aldolase active form is a homotetramer of 33 kDa subunits (Freeze & Brock, 1970; De Montigny & Sygusch, 1996, Sauvé & Sygusch, 2001). Amino-acid sequence comparisons of *Taq* FBP aldolase with the above class II aldolases of known structure, namely *E. coli* fuculose-1-phosphate aldolase, *E. coli* class II A FBP aldolase and 2-dehydro-3-deoxy-galactarate aldolase, yielded respective sequence identities of 18, 27 and 21% and similarities of 42, 52 and 45%. The comparison reiterates that polypeptide folding by *Taq* FBP aldolase is most likely to be homologous to that of the functionally identical *E. coli* class II A FBP aldolase. Detailed sequence analysis of *Taq* FBP aldolase revealed an insertion of 21 amino-acid residues that may be involved in tetramer formation and activity regulation (Sauvé & Sygusch, 2001). The thermophilic enzyme is resistant to high temperatures (>363 K) for prolonged periods as well as to significant concentrations of alcohols and detergent (De Montigny & Sygusch, 1996). These properties make it useful for aldol condensations in organic chemistry (Von der Osten *et al.*, 1989) under conditions where its *E. coli* homologue is unstable.

2. Methods

2.1. Native FBP aldolase from *Taq*

Native protein was expressed and purified by heat treatment followed by two chromatographic steps (Sauvé & Sygusch, 2001). Dynamic light scattering was performed using a DynaPro-801 TC (Protein Solutions) apparatus and analysis has shown the purified protein to be monodisperse and to possess a molecular weight consistent with a tetrameric quaternary structure.

2.2. Expression of the selenomethionine FBP aldolase from *Taq*

The seleno-L-methionine (SeMet) isoform of FBP aldolase of *Taq* was expressed in *E. coli* strain JM109 in the presence of high concentrations of isoleucine, lysine and threonine to inhibit methionine biosynthesis (Budisa *et al.*, 1995). A single colony of *E. coli* JM109 carrying the expression vector of the *Taq* aldolase was used to inoculate 30 ml of DYT with 0.1 mg ml^{-1} ampicillin. This culture was grown at 310 K until the exponential phase was reached, corresponding to an OD at 600 nm of 0.8. Bacterial cells were centrifuged at 3000*g* for 15 min at 277 K. The pellet was resuspended in 15 ml of NMM media (0.4 g l^{-1} NH_4Cl, 0.5 g l^{-1} NaCl, 7.5 g l^{-1} KH_2PO_4 and K_2HPO_4) supplemented with 1 m*M* $MgSO_4$, 21.6 µ*M* $CaCl_2$, 20 m*M* glucose, 7 mg l^{-1} $(NH_4)_2Fe(SO_4)_2$, 10 mg l^{-1} thiamine, 10 mg l^{-1} biotin, 2.9 µg l^{-1} $CuCl_2.2H_2O$, 3.6 µg l^{-1} $MnCl_2.4H_2O$, 2.1 µg l^{-1} $ZnCl_2$, 2.5 µg l^{-1} $Na_2MoO_4.2H_2O$, 60 mg l^{-1} L-selenomethionine, 50 mg l^{-1} of valine, isoleucine and leucine, 100 mg l^{-1} of threonine, phenylalanine and lysine. A 1.5 l culture of supplemented NMM containing 0.1 mg ml^{-1} ampicillin was inoculated with 15 ml of bacteria suspension and was grown for 16 h at 310 K and then supplemented with 500 ml of fresh NMM and ampicillin. When the culture density had reached an OD at 600 nm of 0.8, adding IPTG to a final concentration of 0.5 m*M* induced *Taq* FBP aldolase expression. After 7 h induction, cells were harvested by pelleting at 8000*g* for 15 min at 277 K.

2.3. Purification of selenomethionine protein

The harvested pellet was resuspended in a buffer containing 50 m*M* Tris–HCl pH 7.3, 0.1 m*M* phenylmethylsulfonyl fluoride and 1 m*M* dithiothreitol and lysed by sonication. The resultant suspension was centrifuged at 35 000*g* for 15 min at 277 K. The supernatant was delipidated by lowering its pH to 5.4 with 1 *M* acetic acid and was then centrifuged at 35 000*g* for 15 min at 277 K. The pH of the protein solution was adjusted to pH 7.3 with NaOH and diluted twice with lysis buffer. The *Taq* FBP aldolase was purified by heat treatment at 353 K for 45 min with gentle agitation. Denatured contaminating proteins were removed by centrifugation at 40 000*g* for 20 min at 277 K. The protein sample, containing more than 60% *Taq* FBP aldolase, was concentrated by microfiltration for crystallization purposes.

2.4. Initial screening of crystallization conditions for *Taq* FBP aldolase

The recombinant native protein was concentrated by microfiltration to a protein concentration of ~3 mg ml^{-1} in 10 m*M* Tris–HCl pH 7.3. Higher concentrations of protein resulted in noticeable protein aggregation and precipitation. Initial screening was performed at 295 K by vapor-phase diffusion using hanging drops (Ducruix & Giegé, 1992) in which 2 µl of protein was mixed with 2 µl of reservoir solution using sparse-matrix screens (Jancarik & Kim, 1991) obtained from Hampton Research (Crystal Screens I and II and grid screens). *Taq* FBP aldolase was observed to display a strong propensity to form needle-like crystals in the presence of many precipitating agents such as ammonium sulfate, PEGs of various sizes, MPD, ethanol, methanol and 2-propanol. Two

screening conditions were further optimized for crystal growth: condition I, 1.8 *M* ammonium sulfate, 0.1 *M* MES pH 6.5, 0.01 *M* $CoCl_2$ (condition #25 in Crystal Screen II); condition II, 0.8 *M* ammonium sulfate, 0.1 *M* citric acid pH 4 (condition #1 in the ammonium sulfate grid screen).

2.5. Crystallization condition I

Needles were often observed aggregated into larger clusters. To improve protein crystal growth and crystal morphology, the use of various additives was examined. Of the additives investigated, sodium monolaurate proved to be the most successful. Optimum growth occurred using sitting drops made up initially of 8.75 µl of protein at 1.75 mg ml^{-1}, 1 µl of 2 m*M* sucrose monolaurate and 5 µl of the precipitant solution containing 1.7 *M* ammonium sulfate, 0.1 *M* Tris–HCl pH 7.5 and 10 m*M* $CoCl_2$ equilibrated against 1 ml of the precipitant solution at 295 K. Crystals harvested were cryoprotected in mother liquor to which 20% glycerol had been added prior to freezing in liquid nitrogen.

2.6. Crystallization condition II

Hanging drops consisting of 5 µl of protein solution containing 0.25 mg ml^{-1} *Taq* FBP aldolase and 2 µl precipitant solution consisting of 0.6 *M* ammonium sulfate and 20 m*M* citric acid pH 4 were equilibrated against 1 ml precipitant solution at 295 K. Crystals were cryoprotected in mother liquor supplemented with 15% glycerol prior to freezing in liquid nitrogen.

2.7. Data collection and processing

Diffraction data were collected at 100 K at beamline X-8C of the National Synchrotron Light Source (NSLS) at Brookhaven National Laboratory using a Quantum 4R CCD detector (ADSC). All data sets were processed independently using the programs *DENZO* and *SCALEPACK* (Otwinowski & Minor, 1997).

3. Results and discussion

3.1. Crystals from condition I

Only crystals of native protein were obtained under condition I as shown in Fig. 1. These are rod-like in shape and grow to maximal dimensions of 1.5 × 0.1 × 0.1 mm after 2–3 weeks. A data set was collected at 1.105 Å and a crystal-to-detector distance of 150 mm. The exposure time was 40 s per frame, corresponding to an oscillation angle of 0.66°. Data were collected to 95.4% completeness to within 2 Å resolution. Crystals belong to the monoclinic space group *P*2, with unit-cell parameters a = 99.5, b = 57.5, c = 138.6 Å, β = 90.25°. Assuming one homotetramer in the asymmetric unit yields a V_M (Matthews, 1968) of 3.0 Å^3 Da^{-1}, corresponding to a solvent content of 58.9%. Intensity data was merged with the program *SCALEPACK* (Otwinowski & Minor, 1997) and yielded a linear R factor of 0.061.

3.2. Crystals from condition II

Crystals of the native and SeMet enzyme were obtained under condition II; a SeMet crystal is shown in Fig. 2. Bipyramidal crystals appear within a few days and grow to maximal dimensions of 0.25 × 0.16 × 0.16 mm after three weeks. For the native protein, a data set was collected at 1.215 Å and a crystal-to-detector distance of 190 mm. The exposure time was 200 s per frame, corresponding to an oscillation angle of 0.5°. Intensity data extends to within 2.5 Å resolution and was collected to 95.1% completeness. Merging of the intensity data resulted in a linear R factor of 0.121. Native crystals belong to the tetragonal space group $P4_1$, with unit-cell parameters $a = b$ = 88.8, c = 163.1 Å. Assuming one homotetramer in the asymmetric unit leads to a V_M (Matthews, 1968) of 2.4 Å^3 Da^{-1}, corresponding to a solvent content of 49.3%.

Figure 1
A monoclinic crystal of native *Taq* FBP aldolase of dimensions 1.5 × 0.1 × 0.1 mm grown using condition I.

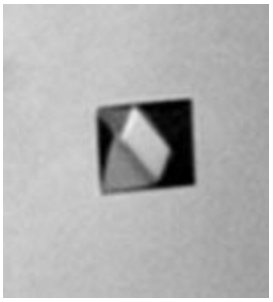

Figure 2
A tetragonal crystal of selenomethionine *Taq* FBP aldolase of dimensions 0.25 × 0.16 × 0.16 mm grown using condition II.

Data for the SeMet derivative were collected in a single pass using inverse-beam geometry at three different wavelengths. An X-ray fluorescence spectrum was recorded and used to select the wavelength optima for MAD data collection. Data were collected at 0.9791 Å (the inflection point of the fluorescence spectrum, f' minimum), 0.9783 Å (the maximum of the fluorescence spectrum, f'' maximum) and 0.9300 Å (the remote high-energy wavelength). Data sets were collected at a crystal-to-detector distance of 240 mm using an exposure time of 70 s and 0.66° oscillation per image. Merging of the intensity data yielded R factors of 0.091, 0.098 and 0.093, respectively, for the anomalous data sets (f' minimum, f'' maximum and remote).

Crystals for the SeMet derivative belong to a different tetragonal space group, $I4_1$, but have very similar unit-cell parameters, $a = b$ = 88.6, c = 164.1 Å. For one homodimer per asymmetric unit, V_M is 2.4 Å^3 Da^{-1} and corresponds to a solvent content of 49.4%. Intensity data extends to 2.6 Å resolution with 97% completeness.

Structural analysis should lead to the determination of the first structure of a class II B FBP aldolase. Based on homology modeling, helices in the class II B aldolase appear to be shorter and it will be of interest to determine to what extent helix length affects $(\alpha/\beta)_8$-barrel structure and whether there are other structural changes related to sequence differences in class II B aldolase structure. Moreover, it will be intriguing to determine whether the cobalt cation in *Taq* FBP aldolase exhibits the same conformational heterogeneity as in *E. coli* aldolase, where two mutually exclusive conformations have been observed for the same zinc cation. We should also be able to gain insight into the role of the 21-amino-acid sequence insertion regarding enzymatic activity, as in the *E. coli* homologue this insertion maps to the DHAP-binding site. The structure should also show which subunit surfaces are involved in tetramer formation and whether the 21-amino-acid insertion sequence (predicted helical secondary structure) is indeed involved in stabilizing the quaternary structure. Lastly, it should be possible to identify the nature of the thermophilic adaptation – additional ion pairs, hydrogen bonds or hydrophobic patches – that results in the enhanced thermostability of *Taq* aldolase and whether greater surface hydrophobicity of the protein explains its high stability in detergents and alcohols.

Research was supported by funding from MRC (Canada). The assistance of Dr Tae-

Sung Yoon in data collection and reduction is gratefully acknowledged. Work was carried out in part at the National Synchrotron Light Source, Brookhaven National Laboratory, which is supported by the US Department of Energy, Division of Materials Sciences and Division of Chemical Sciences under contract number DE-AC02-98CH10886. Assistance by X8-C beamline personnel, Dr L. Flaks, was appreciated.

References

Blom, N. S., Tétreault, S., Coulombe, R. & Sygusch, J. (1996). *Nature Struct. Biol.* **3**, 856–862.

Brock, T. D. & Freeze, H. (1969). *J. Bacteriol.* **98**, 289–297.

Budisa, N., Steipe, B., Demange, P., Eckerskorn, C., Kellermann, J. & Huber, R. (1995). *Eur. J. Biochem.* **230**, 788–796.

Cooper, S. J., Leonard, G. A., McSweeney, S. M., Thompson, A. W., Naismith, J. H., Qamar, S., Plater, A., Berry, A. & Hunter, W. N. (1996). *Structure*, **4**, 1303–1315.

De Montigny, C. & Sygusch, J. (1996). *Eur. J. Biochem.* **241**, 243–248.

Dreyer, M. K. & Schulz, G. E. (1993). *J. Mol. Biol.* **231**, 549–553.

Ducruix, A. & Giegé, R. (1992). *Crystallization of Nucleic Acids and Proteins: A Practical Approach*, edited by A. Ducruix & R. Giegé, pp. 73–98. New York: IRL Press.

Freeze, H. & Brock, T. D. (1970). *J. Bacteriol.* **101**, 541–550.

Hall, D. R., Leonard, G. A., Reed, C. D., Watt, C. I., Berry, A. & Hunter, W. N. (1999). *J. Mol. Biol.* **287**, 383–394.

Haney, P. J., Badger, J. H., Buldak, G. L., Reich, C. I., Woese, C. R. & Olsen, G. J. (1999). *Proc. Natl Acad. Sci.* **96**, 3578–3583.

Izard, T. & Blackwell, N. C. (2000). *EMBO J.* **19**, 3849–3856.

Jancarik, J. & Kim, S.-H. (1991). *J. Appl. Cryst.* **24**, 409–411.

Matthews, B. W. (1968). *J. Mol. Biol.* **33**, 491–497.

Otwinowski, Z. & Minor, W. (1997). *Methods Enzymol.* **276**, 307–326.

Plater, A. R., Zgiby, S. M., Thomson, G. J., Qamar, S., Wharton, C. W. & Berry, A. (1999). *J. Mol. Biol.* **285**, 843–855.

Plaumann, M., Pelzer-Reith, B., Martin, W. F. & Schnarrenberger, C. (1997). *Curr. Genet.* **31**, 430–438.

Rutter, W. J. (1964). *Fed. Proc.* **23**, 1248–57.

Sauvé, V. & Sygusch, J. (2001). In the press.

Von der Osten, C. H., Sinskey, A. J., Barbas, C. F. III, Pederson, R. L., Wang, Y.-F. & Wong, C.-H. (1989). *J. Am. Chem. Soc.* **111**, 3924–3927.

Woese, C. R. (1987). *Microbiol. Rev.* **51**, 221–271.